

Review Article

Graphene as Nanocarrier in Drug Delivery

Federica Valentini^{1,2*}, Andrea Calcaterra², Vincenzo Ruggiero^{3,4},
Mattia Di Giacobbe^{3,5}, Maurizio Botta³, and Maurizio Talamo²

¹Department of Sciences and Chemical Technologies, University of Roma Tor Vergata, Italy

²Inuit Foundation, University of Roma Tor Vergata, Italy

³Department of Biotechnology, Chemistry and Pharmacy, University of Siena, Italy

⁴Hygeia Lab S.r.l, Via della Ricerca Scientifica, University of Roma Tor Vergata, Italy

⁵AlgaRes S.r.l, Via della Ricerca Scientifica, University of Roma Tor Vergata, Italy

*Corresponding author

Valentini F, Department of Sciences and Chemical Technologies, University of Roma Tor Vergata, Via della Ricerca Scientifica 1, Italy, Tel: (39) 0672594889; Fax: (39) 0672594783; Email: federica.valentini@uniroma2.it

Submitted: 12 December 2017

Accepted: 16 January 2018

Published: 19 January 2018

ISSN: 2334-1815

Copyright

© 2018 Valentini et al.

OPEN ACCESS

Keywords

• Graphene; Graphene oxide; Graphene derivatives; Nanocarrier; Drug delivery; Controlled release mechanisms; Nanobiomedicine

Abstract

Pristine Graphene (pG) could represent a new and promising nanomaterial for medicine applications, because it does not catalyze the production of ROS (Reactive Oxygen Species), being in total absence of oxygenated functional groups. In fact, pG either in a dispersed or aggregated form, does not increase mitochondrial oxidant generation or induce apoptosis in lung macrophages, working at room temperature. pG presents another problem due to its thermal instability. In fact, it is very well known that pG spontaneously wrap up forming nanotubes (which result highly toxic for humans, because of their typical asbestos like structures). On the other hand, Graphene Oxide (GO) provokes severe lung injury that persists for more than 21 days after administration. In cultured alveolar macrophages and epithelial cells, GO induces the generation of mitochondrial ROS, by participating in redox reactions with components of the mitochondrial electron transport chains. Several data, described in literature, suggest that all the chemical-physical processes that maintain the nanoscale dispersion of GO is suitable to reduce the potential health consequences of workplace or environmental exposures and likely facilitate emerging graphene-based biomedical applications. Contrary to pG, the rolling up into the nanotube structures is less favored in presence of GO. It follows that, the GO toxicity is only related to the oxygenated functional groups (as primary sources of OH • radical species, O₂⁻ and H₂O₂). However, the functional groups could be deactivated if involved in the formation of stable covalent bonds, which provide the coating of graphenic nano sheets, with suitable biopolymers. The degree and the chemical composition of the oxygenated functionalities results the principal feature, strictly related to the biocompatibility of graphene nano sheets, but also the two-dimensional planar structure (G is a 2D nanomaterial), the nanometer scale dimensions, the large surface area (~ 3000 m²/g) and the exceptional optical properties (as the auto-fluorescence), certainly contribute to design graphene materials, as new potential carrier for drugs. Finally, the high electrical and thermal conductivity and the good antibacterial/antimicrobial properties are not to be neglected for graphene, too. In this review, authors present an up-dated state of the art concerning the recent advances in this field of research. Briefly, this work describes current strategies for the large scale production of G and the surface chemistry modification of graphene-based nanocarriers, their biocompatibility and toxicity properties. At the same, the review reports on the most relevant cases of study suitable to demonstrate the role of graphene and graphene derivatives (GD) as nanocarrier of anti-cancer drugs and genes (i.e. miRNAs). Especially, the controlled release mechanisms (inside the cell compartments) are also mentioned and explored in terms of ΔpH, Δμ (ionic strength variation), chemico-physical mutual interactions, thermal, photo-(i.e. NIR) and electromagnetic induction. Especially the nanodispersion and/or the accumulation/aggregation status of GO, into human cell lines, results mainly pH-sensitive. This pH-activated processes are expected to promote/catalyze targeted therapeutics release in the acidic environment of tumor cells or in intracellular compartments, such as endosome. For this purpose, an important biological factor like blood pH (and ionic strength) are necessary to discuss in the review.

The review also summarizes, future prospects and challenges in graphene derivatives applications for nanobiomedicine, especially in drug delivery field applications.

ABBREVIATIONS

pG: Pristine Graphene; G: Graphene; GO: Graphene Oxide; GD: Graphene Derivatives; CBNs: Carbon Based Nanomaterials; NBCs: NanoBio Composites

INTRODUCTION

The advanced drug delivery systems, combining the ability to improve the therapeutic efficacy and to reduce side effects of drugs represent a challenge for medicine. Nanotechnology offers a wide range of new strategies to produce innovative nanomaterials, suitable for the development of a large number of smart drug delivery systems [1,2], ranging from carbon

based nanomaterials (CBNs) toward metallic nanoparticles and nanobiocomposites (NBCs) materials. Among all nanostructures, carbon based nanomaterials seem to be eligible as nanovector of drugs and therapeutics. Especially, graphene and GD are “metal free” nanomaterials [3], and for this purpose they represent a smart vehicle for the delivery experiments (to perform on both: *in vitro* and *in vivo* systems). Graphene exhibits ananosheet structure that makes easier the translocation of the nanocarrier across the cellular membranes and the cellular compartments. Graphene and graphene derivatives exhibit excellent antibacterial and antimicrobial properties, fundamental aspect to avoid/to minimize the bacterial and microbial infections that could occur during therapeutics deliveries. Several

organic chemistry strategies can be applied on graphene derivatives, to synthesize functionalized and engineered carbon nanoplateforms, suitable to selectively load drugs, RNA sequences, therapeutic agents for interesting nanomedicine applications [4]. Another important aspect is the eco-sustainability of the nanomaterials, in fact graphene and its derivatives are low-impact environmental materials, especially towards end users. Eco-friendly graphene could be obtained by green chemistry approaches from renewable natural sources, using water as solvent. This review is organized on sub headings concerning different synthetic approaches (focusing the attention on the mass industrial production of graphene), the characterization and functionalization of the resulting synthesized products, their chemico-physical and biochemical properties, which render pG and GD eligible as nanocarrier for drugs and therapeutics. Several parameters, as degree and chemical composition of oxygenated functionalities, size and shape, nanodispersion status as function of pH, biochemical features and nanomaterial stability (in cellular compartment environments) are investigated and discussed in relation to the graphene biocompatibility effects, exhibited by pG, GO and GD. For this purpose, several cases of study, are presented and detailed interpreted.

SYNTHESIS AND FUNCTIONALIZATION

There are different strategies to produce graphene nanosheets, having many different features [5], as highlighted on Table 1.

Micro-cleavage and mechanical exfoliation

The Single Layer pG is mainly obtained by mechanical exfoliation, very well known as "scotch tape technique", according to the literature [6], Nobel Prize on Physics, 2010]. Following this strategy, pristine single layer of graphene is obtained by micro-cleavage of the highly oriented pyrolytic graphite, used as precursor. pG does not own oxygenated functional groups and it is not eligible for a covalent/stable loading of drugs, which implies the presence of organic functional groups, to establish covalent bonding/interactions. pG could establish only π - π weak interactions, which are suitable for a controlled and modulated release of the therapeutics. The inner auto-fluorescence exhibited by pG represents another smart feature of this nanomaterial, especially useful for high resolution imaging techniques (for applications in clinical diagnostics). Intrinsic fluorescence properties of graphene provides to avoid further synthetic treatments, to introduce fluorophores dyes into the structure of G, which could generate several problems, as: decrease of the overall yield and the contamination of the pristine materials (due to the use of chemical reagents to bind covalently fluorophores).

When the stability of the nanocarrier/drug composite is strongly required during the delivery in the cell compartments, covalent bonding is needed and, for this purpose, GD should be synthesized, by using mainly chemical and electrochemical liquid phase synthesis, as described in the following sub headings.

In addition, GD results easy to isolate, manipulate and quite stable in cell culture media as well as in physiological medium.

Chemical vapor deposition (CVD)

CVD is one of the most powerful methods to fabricate single

layer of graphene, with a high quality of the resulting materials. Large area SLG samples are prepared by exposing a metal to different hydrocarbon precursors at high temperatures [6a-d]. There are different types of CVD techniques, as: plasma-enhanced CVD, thermal CVD, and hot/cold wall CVD. The graphene growth seems to be organized in two main steps: a) the growth of carbon atoms that nucleate on the metal, after decomposition of the hydrocarbons precursor, and b) the nuclei grow then into large domains. Traditional/conventional gaseous hydrocarbons such as methane, ethylene or acetylene, are used, but recently liquid precursors have also been applied such as hexane or pentane. A very useful and fascinating method for the production of inch-sized single-crystalline graphene has been proposed by Wu et al. [6d and references cited therein]. The authors work with a controlled nucleation method on a Cu-Ni alloy, by locally feeding carbon precursors to a specific position. According to the authors, the use of the specific alloy activated an isothermal segregation mechanism, which resulted in higher growth rates. The final obtained material was a high-quality, 1.5-in. single crystalline graphene, which was synthesized in 2.5h and exhibited a Hall mobility of 10,000–20,000 $\text{cm}^2 \text{V}^{-1} \text{s}^{-1}$ at room temperature.

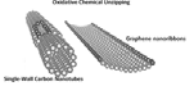
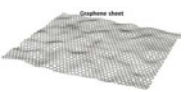
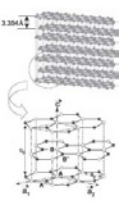
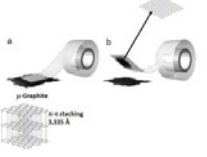


Chemical Synthesis (in liquid phase)

This strategy is carried out in liquid phase, using the very well known Hummer's method [7]. Briefly, this method consist in a chemical procedure applied to generate Graphite Oxide (GO) nanosheets in oxidizing and acidic conditions, realized through the addition of potassium permanganate to a solution of graphite (used as solid precursor), sodium nitrate, and sulfuric acid. Several authors have optimized and modified the first Hummer's method, changing the oxidizing reagents in solutions [8-10] or the starting materials. According to the latter consideration, Cataldo et al. [11,12], reported about the chemical unzipping of Single-Wall Carbon Nanotubes (SWCNTs) and Multi-Wall Carbon Nanotubes (MWCNTs) in a liquid mixture of oxidizing and acidic chemical agents (different from those applied in the conventional Hummer's method). GO nanoribbons and GO nanoplatelets have been fabricated, by the unzipping method, starting from the carbon nanotubes (as solid precursor of graphene derivatives). The great advantage of the chemical synthesis is to produce functionalized graphene derivatives (mainly consist in carboxylic and carbonyl functional groups) in the same step of their synthesis/growth, avoiding post-synthetic functionalization, required by the physical method based on the micro-cleavage. Chemical synthesis increases the hydrophilic character of the graphene, allowing better dispersibility and stability in the most common working media (widely used in Nanomedicine field application). The hydrophilic features improve the interactions (established by electrostatic and Coulombian weak forces) among drugs, genomic material, biomolecules and graphene nanoplateforms. The resulting dispersibility also enhances, promoting the delivery of the carrier/drug composites, into the cellular compartments. The drug release result more efficient, because the electrostatic/Columbian forces are weak enough, allowing the drug to be removed from the nanocarrier.

Electrochemical synthesis (in liquid phase)

The exfoliation of graphene could be successfully reached by applying an electrochemical approach, in a traditional

Table 1: main synthesis strategies to fabricate graphene and its properties.

Synthesis strategies	Experimental Conditions	Shape	Size	Biocompatibility effects
Chemical wet synthesis (mass production in Laboratory)	200 mg of the pristine SWCNT in 200 ml of a mixture of concentrated HNO ₃ /H ₂ SO ₄ in a 1:3 volume ratio followed by 8h of ultrasonic treatment performed at 50 W at 45 C. To reach neutrality, they were washed with distilled water and finally dried in an oven at 100 C.		φ= 22 and 26 nm Diameter range of GO nanoribbons	Lower at low concentration levels Decreases with the concentration values incubated into the normal human cell lines
Electrochemical wet synthesis (mass production in Laboratory)	Oxidative potential regime is applied, ranging from 12-60V by a DC-Supplier tool. The electrolysis bath is made of conventional electrolytes, with a concentration of 0.1-0.5M, in aqueous working medium. The growth time ranging from 1h to 3hours, at R.T.		Width of the sheet: 3μm Thickness: (0.335nm x3) 3 layers (1.005nm)	High at medium/high concentration values incubated in normal human cell lines
CVD Chemical Vapor Deposition (Lowest amount in Laboratory Large amount in industries)	Large area samples can be prepared by exposing a metal to different hydrocarbon precursors at high temperatures. A controlled nucleation method on a Cu-Ni alloy, by locally feeding carbon precursors, provides single crystalline graphene, which was synthesized in 2.5 h.		Thickness: 0.335nm π-π stacking	High Biocompatibility into normal human cell lines
Micro cleavage Mechanical exfoliation (Mass production Laboratory)	In this technique, a piece of graphite undergoes repeated tape exfoliation and is then transferred to a substrate. The same method of Geim and Novoselov, awarded with the Nobel Prize in 2010		The ideal Single Layer of Graphene Thickness: 0.335nm π-π stacking	The Best Metal free nanosheets Single Layer
Mechanical blender wet exfoliation (Mass production Laboratory)	Though the shear rate decreases with the increasing distance from the blade, high shear rate can cover all the holder if a turbulence is fully developed. Therefore, the turbulence is mainly responsible for the full-field high shear rate and thus the exfoliation mechanism of graphite into graphene nanosheets		Single Layer of Graphene Thickness: 0.335nm π-π stacking Double layer (0.335nm x 2)	The Best Metal free nanosheets Single/Double Layer
Biomass solid/wet extraction (Mass Production Laboratory)	Solid/Liquid phases extraction from cellulose, lignin and hemp represent the organic biomass for graphene large scale production		Few layers of graphene (<10 layers)	The Best Metal free nanosheets Single/Few Layers

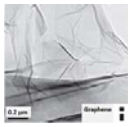
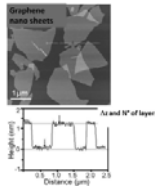
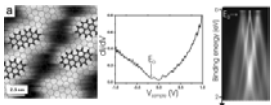
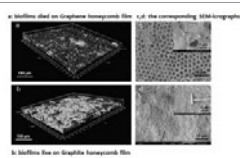
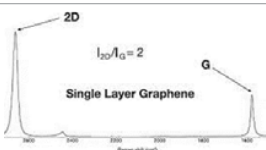
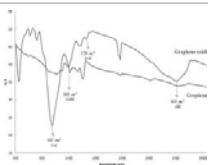
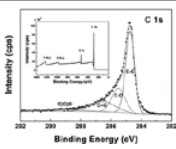
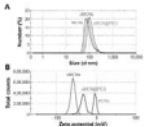
SWCNTs: Single-Wall/Walled Carbon Nanotubes

electrolytic cell. In literature [13], these authors report about the electrolytic exfoliation (performed in different inorganic salts, as: (NH₄)₂SO₄, Na₂SO₄, K₂SO₄, etc.) combined with ions intercalation into graphite working electrodes. Exfoliation/intercalation mechanisms, carried out in these electrolytes leads to graphene with a high yield (>85%, ≤ 3 layers), large lateral size (up to 44 μm), significant oxidation degree (a C/O ratio of 17.2), and a remarkable hole mobility of 310 cm² V⁻¹ s⁻¹[13]. The described electrochemical exfoliation shows great promise for the industrial-scale synthesis of high-quality mass production graphene for numerous advanced applications. In addition, the

electrochemical techniques provide a versatile approach, simply modifying the electrolytic bath, according to the final applications. Working with the electrochemical synthesis, no single layer of graphene is obtained but consistent amount of double and multi-layers (≤ 5 layers) of graphene oxide (no pristine, when authors work at oxidative range of potential values).

An Electrophoretic Deposition Process (EPD) represents another electrochemical exfoliation technique, where the graphene sheets are synthesized and simultaneously oriented, by the presence of an external electric field (i.e electrophoresis mechanism). The carbonaceous nanomaterial precursors are

Table 2: Main information by applying the characterization techniques for SLG.

Techniques	Data/results	Qualitative analysis	Quantitative analysis	Biomedical applications
Microscopic techniques for morphological/topographic characterization studies				
HR-TEM/EDAX		Sheets width	Semi-quantitative/EDAX for metal	Metal free nanomaterials for cytotoxicity
AFM		Sheets width and area	Thickness for N° of layers	Shape and orientation involved in the cell membrane crossing
STM/STS		Atomic resolution hexagon	Band gap; Bias V_{cond} vs. V_{val}	Alignment and electronic properties for cell membrane crossing
CLSM		Internalization in cells	Fluorescence quantitative analysis	Specific and selective identification of nanomaterials in the inner cellular compartments
Spectroscopic techniques for structural characterization studies				
Raman		Fingerprint of SLG $I_{2D}/I_G=2$	I_D/I_G degree of functionalization	Molecular inner cell interactions
FTIR		PG exhibits a featureless FTIR spectrum	Identification of functional groups	ROS pathways for cytotoxicity events
XPS		Chemical-shift of carbon atoms	% atomic quantification/%(w/w)	ROS pathways for cytotoxicity events
Z-potential/DLS		Graphene sheets surrounded by solvent	$\Phi_{Hydrodynamic}$: electrostatic potential	Electrostatic interactions in cells

DLS: Dynamic Light Scattering

dispersed in organic solvents (also in water medium), using constant voltage conditions. Uniform graphene-based layers can be also deposited on three-dimensional, porous, and even flexible substrates, applying a template synthesis approach. In general, electrophoretically deposited graphene layers show excellent properties, e.g., high electrical conductivity, large surface area, good thermal stability, high optical transparency, and robust mechanical strength. EPD also allows the production of functional nanocomposite materials, e.g., graphene combined with metallic nanoparticles, with other carbonaceous materials (e.g., carbon nanotubes) or biopolymers, leading to novel nanomaterials with

enhanced optical, electrical and biocompatible features (suitable for *in vitro* and *in vivo* test/assay).

Mechanical blender based exfoliation in liquid phase (in liquid phase)

Coleman et al. [14], report about the development of industrially scalable methods to produce large quantities of defect-free graphene, different from those described above, in the full text. Coleman et al. [14], show that high-shear mixing of graphite in suitable stabilizing liquids results in large-scale exfoliation to give dispersions of graphene nanosheets. X-ray photoelectron

spectroscopy and Raman spectroscopy show the exfoliated flakes to be unoxidized and free of basal-plane defects. Coleman et al. [14], developed a simple model that shows exfoliation to occur once the local shear rate exceeds 104s^{-1} . By fully characterizing the scaling behavior of the graphene production rate, the authors show that exfoliation can be achieved in liquid volumes from hundreds of milliliters up to hundreds of liters and beyond. The graphene produced by this method performs well in applications from nanobiocomposites to conductive coatings.

Coleman's approach is not the only one strategy but different exfoliation techniques based on a mechanical exfoliation mechanism [15], can provide fruitful information on how to efficiently achieve high-quality graphene. This review highlights the recent progress on mechanical exfoliation for graphene production during the last decade. The emphasis is set on the widely used sonication method with the latest insight into sonication-induced defects, the newly explored ball milling method, the fluid dynamics method that has emerged in the last three years, and the innovative supercritical fluid method.

Biomass extraction of graphene network: an environmental bioremediation approach

Chen et al. [16], demonstrate that it is possible to fabricate large amounts of few-layer graphene by an eco-friendly and eco-sustainable method that uses biomass waste as the precursor of graphene derivatives. Wheat straw was selected as the starting material [17], because of its enormous worldwide output (about 350 million tons per year all over the world). This biomass has attracted enough attention for the production of nanomaterials, such as nanosilica [18,19], activated carbon [20,21], and especially graphene [16]. Feng et al. [16], report about the great possibility to successfully convert wheat straw into graphene nanosheets, combining the hydrothermal and graphitization process. Applying this method, high-quality, few-layer pristine graphene with high graphitization, graphite-like interlayer spacing, and moderate meso-porosity can be prepared. Moreover, this process is simple, highly efficient, environmentally benign, cost-effective, and catalyst-free.

Ojha et al. [22], synthesize graphene-like activated and non-activated carbon sheets from starch. Similarly, authors have also synthesized activated carbon nanostructures from natural sources like jute and rice husk. The chemical-physical features, the biochemical properties (mainly related to the biocompatibility) and the supercapacitor effects of these carbon nanomaterials have been investigated and compared with that exhibited by graphene oxide and reduced graphene oxide. Sharma et al. [23], report about four different biomass derived green and sustainable solvents namely levulinic acid (LA), ethyl lactate (EL), γ -valerolactone (GVL) and formic acid (FA) only LA was found to exfoliate graphite to single and few layered graphene sheets. During exfoliation, the formation of LA crystals embedded with single layered graphene sheets was observed. The process is scalable and the solvent can be recovered and reused in five subsequent cycles of exfoliation for the large scale production of graphene sheets.

Shams et al. [24], describe a simple, eco-friendly and scalable method of obtaining graphene from dead camphor

leaves (*Cinnamomum Camphora*) using one-step pyrolysis. Under flowing nitrogen atmosphere, dead camphor leaves were heated to 1200°C at $10^{\circ}\text{C}/\text{min}$ and then cooled down to room temperature. With the help of π - π interaction with D-Tyrosine and centrifugation, we were able to separate few layer graphene from the final pyrolytic components. Characterization studies reveal the presence of 7 layers of graphene. It is possible to affirm that this novel eco-friendly and eco-sustainable approach will motivate the search for a new way for synthesis of graphene sheets from reproducible natural products.

CHARACTERIZATION OF THE CHEMICAL-PHYSICAL PROPERTIES OF PG AND GD

The chemical-physical and mechanical-engineering studies are essential to characterize the presence of pristine graphene and graphene derivatives, in synthesised samples. The main techniques, dedicated to the graphene characterization are highlighted in this review, with their useful information about the new synthesized materials. Each technique provide useful parametersto identify graphene and graphene derivatives, as reported below in the text (Table 2).

Raman spectroscopy

Raman spectroscopy and imaging (μ -Raman) represent powerful, noninvasive method to characterize graphene and related materials. Several use fulin formation such as disorder, edge and grain boundaries, thickness, doping, strain and thermal conductivity of graphene can be obtained working with Raman spectroscopy. In particular for graphene, the Stokes phonon energy shift caused by laser excitation creates two main peaks in the Raman spectrum: G (1580 cm^{-1}), a primary in-plane vibrational mode typical of graphite, and 2D (2690 cm^{-1}), a second-order overtone of a different in-plane vibration, D (1350 cm^{-1}), that represents the defects band [25]. The spectrum changes as the number of graphene layers increases, presenting a splitting of the 2D band into an increasing number of modes [25]. The G band also exhibits a red shift from number of layers [26]. Thus, for AB-stacked graphene, the number of layers can be obtained from I_{2D}/I_G ratio intensity, as well as the position and shape of these bands [27]. Using I_D/I_G , one can use Raman spectra to characterize the level of disorder in graphene. As disorder in graphene increases, I_D/I_G displays 2 different spectral profiles. In presence of "low" defect density, I_D/I_G increases because a higher defect density creates more elastic scattering. This occurs up to a regime of "high" defect density, at which point I_D/I_G begins to decrease as an increasing defect density results in a more amorphous carbon structure, attenuating all Raman peaks [28].

High resolution-transmission electron microscopy/energy dispersive X-Ray analysis (HR-TEM/EDAX)

The morphology/topography and crystalline structure of pG, GO and GD having different degrees of oxidation/functionalization was analyzed using HR-TEM/EDAX (High Resolution-Transmission Electron Microscopy/Energy Dispersive X-Ray Analysis) and selected area electron diffraction (SAED) pattern, respectively. Graphene samples possess a sheet morphology exhibiting different optical transparencies and different sizes. This is probably due to the number of layers present in the stacked

structure of GO/GD. The samples with less oxygenated functional groups show multi layers of graphene, because of the presence of the hydrophobic interactions (responsible for the mutual π - π aggregation among the G layers). According to this, multi layers are less transparent (if compared with the single layer, double and few layers of graphene) and exhibit large size (associated to the aggregated layers). HR-TEM provides an important information on the statistical distribution of nanosheets sizes.

HR-TEM measurements shows that the sheets morphology, their dimension and the optical transparency are strictly dependent on the level of oxidation and the functionalization degree, that occur during the exfoliation strategies.

The SAED pattern is used to characterize the crystalline nature of nanosized materials. The SAED pattern of all the samples possess clear diffraction spots with a six-fold pattern that is consistent with the hexagonal lattice of graphene [29]. This means that the graphitic AB stacking order is preserved in the lattice even after oxidation treatments of graphite precursor to do graphene final product. No diffraction pattern is obtained for the over-oxidized carbon samples. The absence of the hexagonal spots of graphitic nature indicate that the oxygenated functional groups are not organized in super-lattice type ordered arrays [30].

EDAX provides useful information about the elemental analysis/microanalysis of the graphene derivatives. This is only a semi-quantitative approach.

Atomic force microscopy (AFM) and scanning tunnel microscopy/scanning tunnel spectroscopy (STM/STS)

Atomic Force microscopy provide information about the regular shape of graphene and graphene oxide sheets (symmetric and asymmetric sheets), its area and thickness (histogram of the z heights). Thickness provide the number of the layers for multilayer of oxidized graphene sheets that are integer multiples of a layer height ~ 0.67 nm (corresponding to the π - π stacking). Similar properties attributed to wrinkles (the wrinkles have variable heights that are approximately 1.0-4.5 nm above the oxidized graphene sheet) and folds, albeit at a more magnified scale, were also observed during studies with STM (Scanning Tunneling Microscopy). The atomically resolved STM topography reveals the position of oxygen on the top of the graphene oxide sheets. The known size of the ideal single layer of graphite lattice, we estimate the size of the unit cell for the GO lattice, that corresponds to 0.284 nm by 0.420 nm. This agrees well with the observed periodicity of (0.273 ± 0.008) nm (0.406 ± 0.013) nm from the atomically resolved STM image [31]. The atomically resolved lattice structure is not observed at all regions across the oxidized graphene sample (GO), leading to the conclusion that other regions may contain several oxygenated functionalities, mainly carboxylic groups (COOH in GO). STS provides information on the electronic conductivity of graphene and graphene derivatives. From the $I(V)$ plots, a clear suppression of current near zero bias is detected in the case of oxidized graphene. Since dI/dV at low bias is proportional to the local density of electronic states (LDOS), the dI/dV data show a measurable suppression in the LDOS for oxidized graphene that extends ± 0.1 V about zero

bias. The corresponding plots $\log_{10}[|I|]$ vs. V_{bias} , clearly shows the presence of a band gap in oxidized graphene (GO) of 0.25 eV. This means that, increasing the defects density (i.e. the oxygenated functionalities), GO becomes insulating materials, if compared with reduced graphene and also the ideal single layer of graphene.

Confocal laser microscopy (CLSM)

CLSM represents a powerful tool for high resolution imaging of nanomaterials incubated into human cell lines. The excellent optical properties of graphene [32], offer a great advantage to detect graphene into the human cell lines, avoiding the labeling pre-treatments, by using fluorophores (avoiding to lose material and to contaminate the samples). In fact, graphene exhibits auto-fluorescence without optical labeling and also the total internal fluorescence reflection signal. These data demonstrate that graphene is eligible for the high resolution imaging based technologies to apply in medical diagnosis [33]. Among all the optical features, the absorbance of Graphene exhibited on UV-vis-NIR spectral region, represents a powerful tool to quantify the loading of drugs, on graphene nanocarriers (by calibration curves). An official quantification of the drug loading on Graphene vectors, is also achieved by a traditional mass spectrometry technique, specific for solid samples; as FAB (Fast Atom Bombardment).

X-Ray photoelectron spectroscopy (XPS)

The chemical shift of carbon atoms in graphene samples is also investigated by the XPS spectroscopy. In a typical XPS spectrum of graphite, only a peak, corresponding to C-C stretching at 284.5 eV and indicating the absence of any oxygenated function groups [34], is detected. Increasing the oxidation degree, the intensity of the C-C peak, due to the sp^2 carbon bond in graphite, gradually decreases and an increase in intensity of new peaks (sp^3 oxygenated carbon atoms), related to the presence of oxygenated functional groups, as: hydroxyl, carboxyl and epoxy groups are clearly evident in the XPS. The sp^2/sp^3 ratio represents an important quantitative parameter to identify by using XPS technique and this ratio decreases with increasing of the oxidation level in graphene and graphene derivative samples.

XPS provides useful information to combine with Raman analysis and FTIR. Spectroscopy (this latter, very well known to identify the oxygenated functionalities of the oxidized carbon based nanomaterials).

XPS and EDAX also provide microanalysis/compositional analysis, useful for the identification of the minimum chemical formula ($C_xH_yO_z$, see Fig X) and its corresponding average molecular weight (MW). FAB can be able to confirm the MWs of graphene derivatives and GO, related to their corresponding $C_xH_yO_z$.

Z-POTENTIAL MEASUREMENTS

This measurement is highly performance when pG/GD samples are dispersed in liquid phase, to obtain information on the electrical charge distribution/density, present on the graphene surfaces. The electrostatic charge density on functionalized graphene sheets enhances the electrostatic interactions between graphene and the most common polar working liquid medium,

resulting in very well nanodispersions. A good operational and long term stability represent a key point to study the cytotoxicity and biocompatibility of new nanostructured materials (for drug delivery, drug discovery and gene transfection experiments), incubated into normal human cell lines.

Generally, Z potential measurements are combined with Dynamic Light Scattering (DLS) analysis to define the size/dimensions of nanosheets, when they are surrounded/solvated by the solvent/liquid working medium. In the particular case of graphene sheets, DLS is not suitable for sizes identification because the associated algorithm for data processing is closely related to spherical particles.

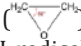
After the description of the main characterization tools for the identification of graphene sheets, in the next paragraph a detailed overview concerning the Biocompatibility features of the new graphene derivatives, are also reported. This property is fundamental to apply GO and GD as new carriers in nanomedicine.

BIOCOMPATIBILITY STUDY OF PG AND GD

The application of pG, GO and GD in nanomedicine, implies that biocompatibility of these new carbon based nanomaterials is demonstrated, both *in vitro* and *in vivo* tests [35]. Toxicity of graphene could depend on many factors like size, shape, surface chemistry, dose, duration and the graphene interactions with the biological working medium. The physico-chemical properties of graphene play a key role in toxicity prediction, as reported in this review, describing different cases of studies, below in the full text.

Several authors, in literature [36], affirm that GO and GD induce (*in vitro* and *in vivo* tests) the production of the reactive oxygen species (ROS), Figure 1. These latter are responsible for the activation of the inflammatory responses and the apoptotic pathways. ROS include the superoxide anion (O_2^-), hydrogen peroxide (H_2O_2), and hydroxyl radicals (OH^\bullet), which exhibit inherent chemical reactivity toward different biological targets.

Recently, another GO based nano sheet material, called as PbS/Ro-GO/PANI nano/microcomposite (roll-graphene oxide (Ro-GO), polyaniline (PANI) nano/microparticles, and PbS nanoparticles) [36b], could be responsible for ROS induced pathways, not only for the presence of oxygenated groups in GO but also for the polymeric radicals, which is due to the polyaniline.

ROS is mainly associated with the principle of oxidative stress, which induces pathology and diseases by damaging lipids, proteins, and nucleic acids. Considering the specificity of ROS toward their molecular targets, the compartmentalization of ROS production within cells is an important parameter, useful to establish if an oxidative damage or a redox signaling, occurs. Accordingly, both the chemical composition of ROS and it's local concentration determine whether redox signaling or oxidative stress induced diseases/disorders occurs. The chemical composition is essential to understand the cytotoxic effects, provoked by reduced graphene and oxidized graphene nano sheets, described above. Reduced graphene could contains on its surface, edges and sides several ethers (C-O-C), epoxic () and alcoholic groups. Mainly alcohols can generate OH radical species, provoking ROS toxic pathways, cinetically faster than that generated by the graphene oxide derivatives. GO and GD, mainly exhibit carboxylic acids (C(=O)OH) if compared reduced graphene, which are less reactive toward the OH^\bullet production. In all cases, pG, GO, PbS/Ro-GO/PANI nano/microcomposite, GD and reduced graphene, the toxicity effects seem to be significantly minimized and reduced when graphene is embedded into a biopolymeric matrices [37]. Also for pG (without functional oxygenated groups) is recommended the biopolymer coatings, because the spontaneous wrap up forming nanotubes, can be avoided (because the edges and sides of graphene sheets, which represent highly recative defects, could be completely protected and deactivated by the presence of polymeric spacer arms).

According to these considerations, Duch, et al. [38], demonstrate that the covalent oxidation of graphene (that occur in

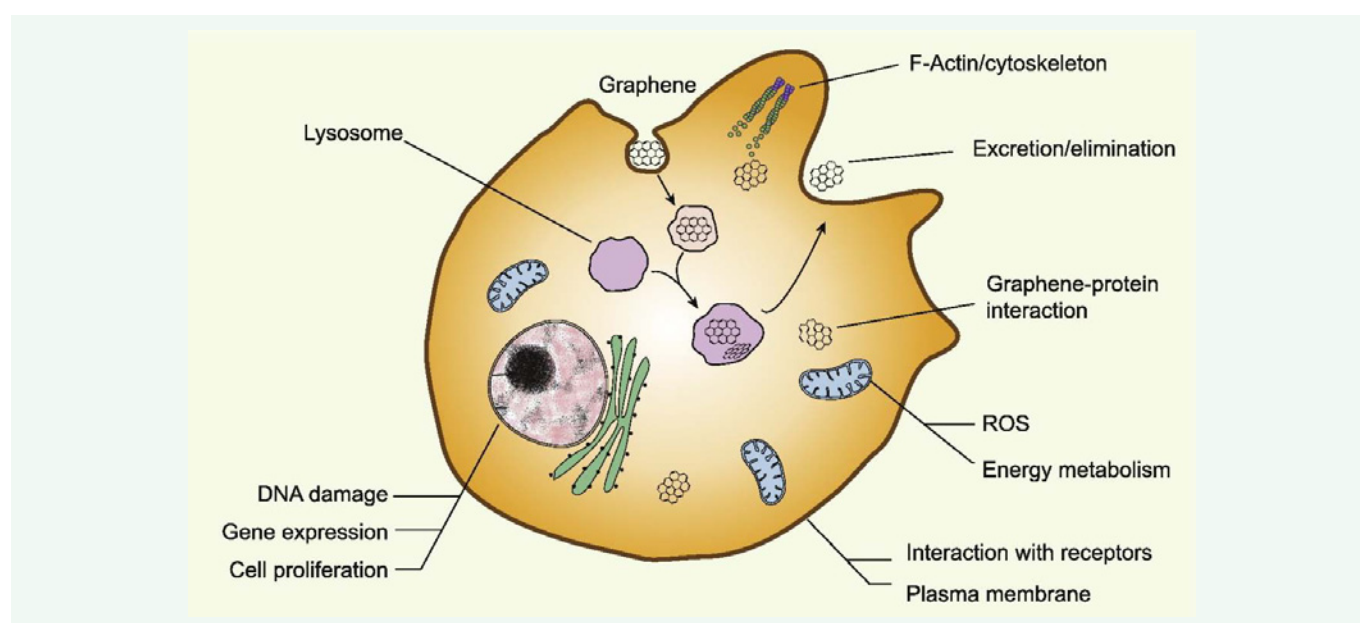


Figure 1 This picture summarizes the recent progress in understanding mainly the interactions between graphene and cells.

presence of GO and GD having oxygenated functionalities suitable to establish the covalent bonding with the drugs, therapeutics and biomolecules) provokes the pulmonary toxicity. The same authors, suggest to apply graphene entrapped in biopolymeric films because in this way, a safe handling of graphene nanosheets, can be successfully reached and biomedical applications, could be performed.

When GO, GD are added (as inorganic filler, up to 1.0 wt. %) in biopolymer matrices (for example, in the ultrahigh molecular weight polyethylene/UHMWPE) to fabricate nanocomposites (called GO/UHMWPE), several parameters of the polymers, significantly improve. The hardness of the pure/native UHMWPE gradually improves but also the polymer yield strength (this latter improves, but slightly). According to these results, Chen et al. [39], demonstrate that MC3T3-E1 cell lines attach very well on the nanocomposite surfaces, and the presence of the graphene filler does not affect the cell morphology and viability. The resulting GO/UHMWPE nanocomposites show improved mechanical properties and significant biocompatibility toward cellular lines, and for this purpose, it is eligible for nanomedicine application field.

Xu et al. [40], report about the mechanism of GO responsible for the toxicity. GO induce platelet depletion, pro-inflammatory responses and pathological changes of lung and liver in mice. Xu et al. [40], explain how to improve the biocompatibility of GO and GD, several different nanocomposites have been synthesized.

Poly(acrylamide)-functionalized GO (GO-PAM), poly(acrylic acid)-functionalized GO (Go-pAA) and poly(ethylene glycol)-functionalized GO (GO-PEG) have been fabricated and tested in vitro and in vivo assay. Among all these nanocomposites, GO-PEG and GO-PAA provide less toxicity if compared with GO and other GD. GO-PAA results the most biocompatible nanocomposite, in both *vitro* and *in vivo* assays. This difference in terms of biocompatibility could be due to the different compositions of the protein corona, especially immunoglobulin G (IgG), as affirmed by Xu et al. [40]. IgG seem to be responsible for the interaction and cellular uptake, the extent of platelet depletion in blood, thrombus formation under short-term exposure and the pro-inflammatory effects under long-term exposure [41].

Recently, Valentini et al. [42], study GO cytotoxicity in Neuroblastoma (both: SK-N-BE(2) and SH-SY5Y) cell lines, measuring cellular oxidative stress (Figure 2), mitochondria membrane potential, expression of lysosomal proteins and cell growth. GO uptake and cytoplasmic distribution of nano sheets were studied by Transmission Electron Microscopy (TEM) for up to 72 h. In SH-SY5Y cells, ROS production increases after 4 h of GO incubation compared with the controlsamples, to reach the maximum value at 24 h and then, decreases at 48 and 72 h, respectively. The increase in ROS provokes the decrease in JC1 ratio (JC1 dye ratio, which is as indicator of mitochondrial potential, see Figure 2). At 48 h, TEM micrographs demonstrate mitochondrial swelling and disorganization in cell lines. GO

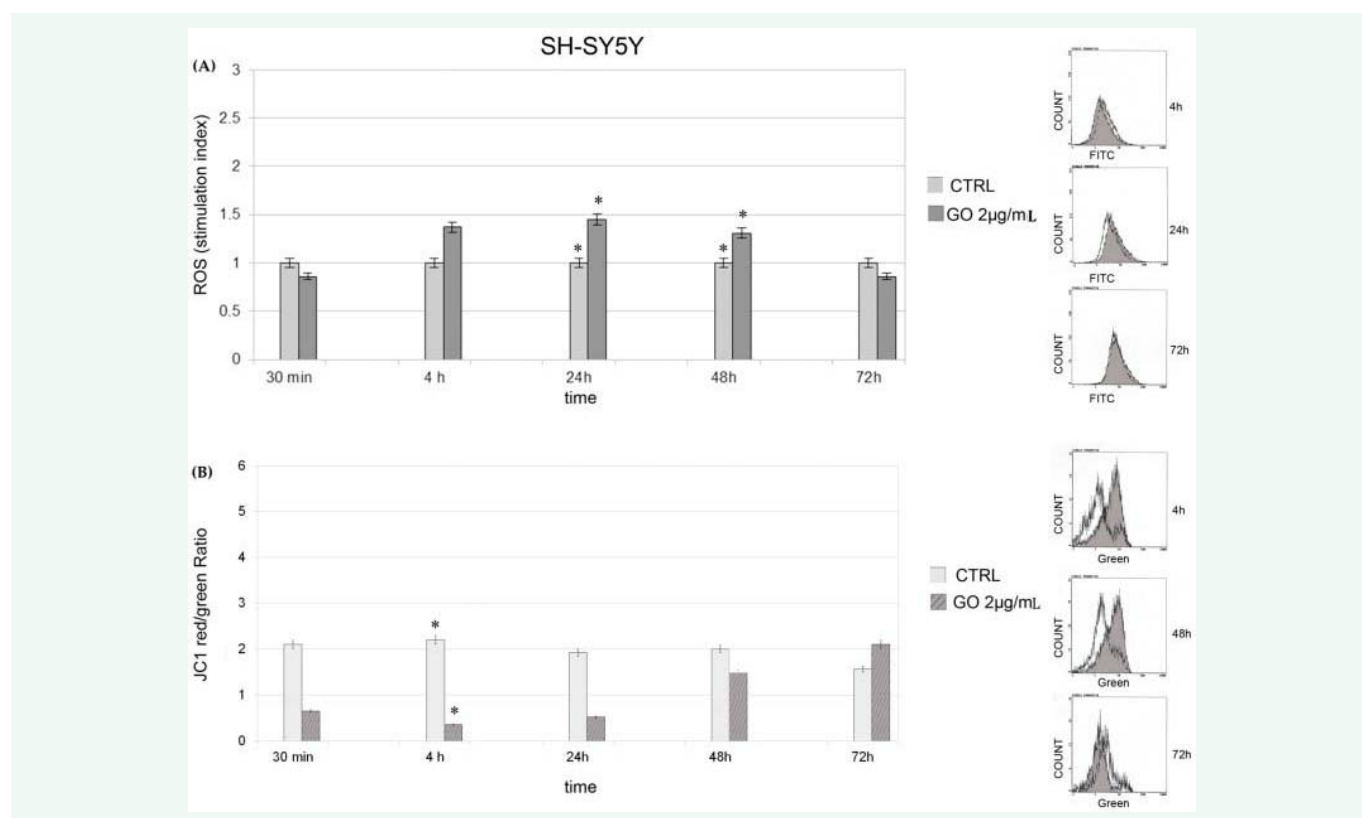


Figure 2 (A): ROS production in SH-SY5Y cells at different times of GO exposure. Data are the mean \pm SD of three different experiments. On the right of the panel, there are indicative fluorescence peaks of control cells and GO treated cells at indicated times. Grey peaks refer to GO treated cells. * $p < 0.05$ for each exposure condition compared to unexposed control (CTRL). (B) JC1 dye in SH-SY5Y cells at different times of GO exposure. On the right of the panel, there are indicative peaks of green fluorescence.

nanoribbons at low concentrations and for 72 h of exposure induce autophagy in neuroblastoma cell lines. This evidence is confirmed by the presence of cytoplasmic vacuoles and by the induction of the lysosomal protein LC3 and beclin, which represent important markers of autophagy. Autophagy is a multistep process which starts with the assembly of the double membrane autophagosome, that entraps a part of cytoplasm and organelles. Valentini et al. [42], also provides the first evidence that cells respond *in vitro*, directly and within hours, to low doses of GO by promoting vacuolation and mitophagy. Moreover, GO incubated cells over-expressed both the early marker of autophagosomes beclin and the late LC3 II phagolysosome marker. The mitophagy marker BNIP 3 is more strongly expressed at 48 h of GO incubation time, and its expression decreases at 72 h. This confirms the existence of compensatory mechanisms that occur after cells have destroyed damaged mitochondria. In fact, Mari et al. [42], show that in neuroblastoma cell lines, GO induces initial oxidative stress and mitochondrial damage. Treated cells respond by activating the autophagic/mitophagic process to repair the damaged proteins and mitochondria. Execution of autophagy/mitophagy starts at 24 and continues up to 72 h, after that cells recover and continue to grow. A possible explanation of this effect, observed on Neuroblastoma (both: SK-N-BE(2) and SH-SY5Y) cell lines, seems to be related to the lowest concentration of GO incubated in cells, that guarantees the highest nano scale dispersion, minimizing the chemical interactions among the oxygenated functional groups (because of which radical species could be formed).

For this reason, authors suggest that the GO nanoparticle can be used for therapeutic delivery to the brain tissue with

minimal effects on healthy cells. On the next paragraph, several cases of studies concerning the role of different kind of graphene derivatives have been reported and described, in details.

GRAPHENE AS NANOCARRIERS FOR ANTI-CANCER DRUGS: SOME CASES OF STUDIES

In this paragraph, authors described the most recent representative cases of studies, where pG or GO/biopolymers nanocomposites and GD, are applied for drug delivery.

The first case of study

Chauhan et al. [43], reports about gold nanoparticles (AuNPs) decoration of GO surfaces, previously functionalized with Folic Acid (FA) as a new carrier suitable for active tumor targeting of model anti-cancer drug (DOX). The resulting AuNPs composite-folate conjugated graphene oxide (FA-GO@Au) nano-platforms result Near-Infrared (NIR) sensitive, exhibiting an efficient release of DOXA and also of the ionic gold from the FA-GO@Au surfaces. Especially, release studies (Figure 3, with or without NIR exposure) showed the effects of irradiated conditions on the release profile of both Dox and Au from the Dox*FA-GO@Au nanohybrid. Only Dox release was significantly influenced by the pH in the simulated body release environment. With a non-linear pseudo order release mechanism of Dox, around 10% higher release was detected at pH 5.3 value, whereas the release of Au content, at different pH values, resulted insignificant. The pH dependence of the Dox release pattern can be attributed to the pH-solubility effects, that increase solubility of Dox (weak amphipathic base, pKa 8.3) and control the mass transfer process occurring in the release media. In this way, the proposed

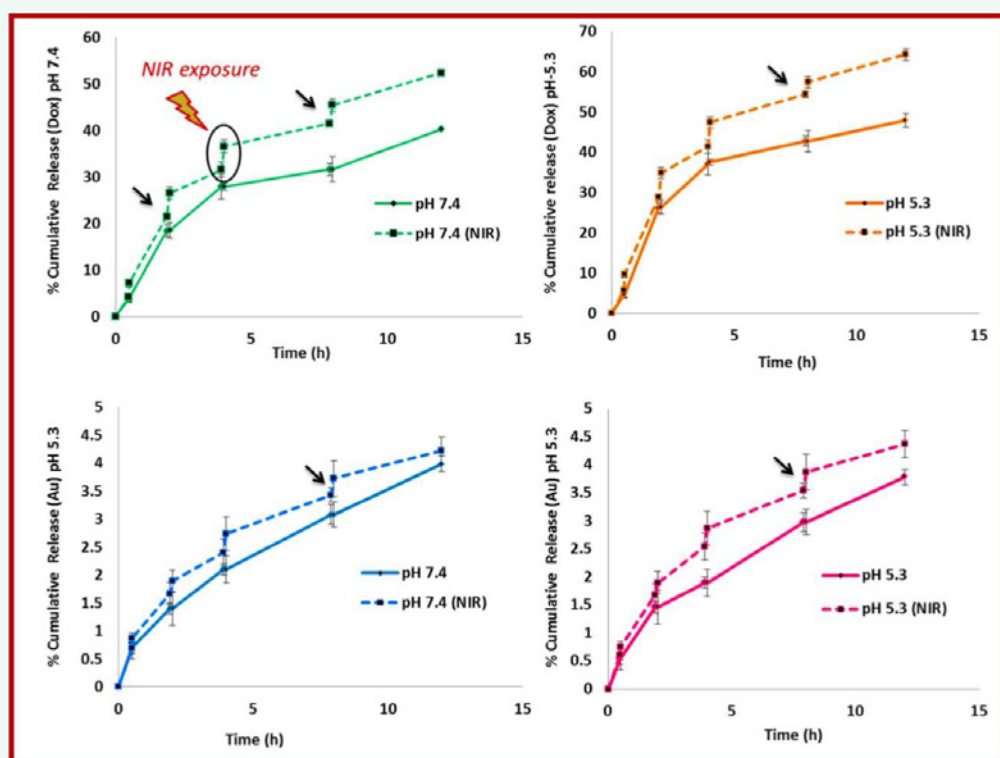


Figure 3 Release profile of Dox and Au from Dox*FA-GO@Au at different pH conditions with or without NIR exposure.

nanohybrid strategy could be able to localize the drug release in slightly acidic endosomal environment, characterizing the cancerous cells. Effect of NIR exposure on Dox*FAGO@Au nanohybrid can be easily seen in the release patterns (dotted lines, on Figure 3) of both Dox and Au, at 12h of exposure time.

Delivery of drugs and AuNPs in the cells is enhanced after NIR localized exposure, resulting in a highest efficiency of tumor management. Especially, Chauhan, et al. [43], describe that there are important evidences *in vitro* and *in vivo* studies, concerning substantial tumor regression in solid tumor model in BALB/c mice and NIR exposure induced photo-thermal effects. Consequently, authors declare that if NIR induces photo-thermal effects, NIR could be used as an efficient tumor-targeting tool. This NIR based nano-hybrid graphene derivatives provides an accurate strategy for targeted chemotherapy and photo-thermal tumor ablation.

The second case of study

Tian et al. [44], describe the fabrication and application of a new nanovehicle conjugated with pegylated folate, suitable for targeted delivery of anticancer drugs and also for fluorescein-labeled peptides, this latter particularly useful in the case of self-monitoring *in vitro* and *in vivo* test. GO sheets have a dimension about 100 nm and a topological height of 1.0 nm, as confirmed by atomic force microscopy, suggesting the presence of a single layer sheet. After conjugation with FA-PEG (pegylated folate) and PepFAM (fluorescein-labeled caspase-3-specific substrate peptide (CALNNDEVDK-FAM, PepFAM), the topological height of nanovehicle reaches the value of 7.5 nm. The zeta potential of FA/Pep/GO nanovehicle was determined to be -20.7 ± 0.41 mV, demonstrating its good stability in aqueous solution.

Flow cytometric assays show that nanovehicle is suitable to deliver and to selectively release drugs into the folate receptor high-expressed cancer cells, providing high therapeutic efficiency to cancer cells. In addition, confocal fluorescence imaging (combined with Confocal Laser Scanning Microscopy (CLSM)) is able to detect the drug-induced cancer cell death, recording the modification of the fluorescence output signal, corresponding to the fluorescein activated by caspase-3, in this specific case of study. The target delivery of drugs and the self-evaluation of therapeutic efficiency are both carried out by living imaging in tumor-bearing mice, providing copious applications of this new theranostic tool *in vivo* systems and also a smart opportunity for accurate and precise cancer treatment base therapies. The apoptotic FAM fluorescence at the tumor region, could be quantified after 24-h injection and the intensity increased along with time for the FA/CPT/Pep/GO (where CPT is camptothecin, a potent topoisomerase I inhibitor) treated mice. After 72-h injection, fluorescence was specifically observed in tumor tissue over other normal organ tissues including heart, liver, spleen, lung and kidney. High FAM fluorescence signals were also recorded in the tumor slice stained with Hoechst, demonstrating the targeted cancer treatment and therapeutic self-monitoring. For the CPT/Pep/GO or FA/Pep/GO treated mice, the FAM fluorescence was less intense than in the tumor region and tumor slice, after 72-h post-incubation time. This result could be due to the lack of FA targeting or drug, confirming the feasibility of FA/Pep/GO nanocarrier for *in vivo* drug delivery and self-evaluation of therapeutic efficiencies.

The third case of study

Dong et al. [45], report about a multifunctional nanocomposite, fabricated by using poly(L-lactide) (PLA) and polyethylene glycol (PEG)-grafted Graphene Quantum Dots (GQDs). The functionalized GQDs (f-GQDs) is able to carry out the intracellular microRNAs (miRNAs) imaging analysis and simultaneously to perform gene delivery for enhanced therapeutic efficiency (Figure 4). The highest surface area, exhibited by f-GQDs represents a great advantage to combine agents (IP and ASODN) (fGQDs/IP/ASODN), targeting miRNA-21 and the survivin gene, to improve the gene therapeutic efficacy. As shown in Figure 4, the cells transfected with f-GQDs/IP/ASODN exhibit a cell viability of 68%, lower than that exhibited by cells transfected with f-GQDs loaded with either IP (f-GQDs/IP), having a cell viability of 82% or ASODN (f-GQDs/ASODN), with a cell viability of 76%. These data demonstrate that the combination of specific gene-targeting agents was essential for induction of better inhibition of cancer cell growth.

GQDs have excellent stability in aqueous solution and also in body medium or serum (excellent conditions for medicine field applications). This behaviour is due to the hydrophilic PEG and PLA polymeric electrically charged chains, which are able to improve the stability of the resulting nanocomposites material into the aqueous phase and/or in physiological working medium. The PL intensity exhibited good stability in acid solution and neutral solution (pH ranging from 3.0 to 7.0), with only a slight decrease compared to the intensity in alkaline solution (pH 9.0). The fluorescence quantum yield of f-GQDs, quantify by using quinine sulfate, as a standard reference compound, results of 6.2%, quite similar to that exhibited in the case of the hydrothermal GQDs, reported previously in literature. Moreover, the time-resolved fluorescence spectrum, measured with an excitation wavelength centred at 320 nm, showed that the fluorescence lifetime (of as-prepared f-GQDs) results of 4.00 ns. The high fluorescence performances, in terms of long-range stability for f-GQDs over a broad pH range, is vital for biomedical investigations.

In vitro cell experiments demonstrate that f-GQDs exhibits excellent biocompatibility, lower cytotoxicity, and protective properties (if compared with pristine materials, without functionalization). In HeLa cell line (used as a model), Dong et al. [45], discover that f-GQDs effectively deliver miRNAs and for this purpose, it is eligible for intracellular miRNAs imaging analysis and regulation. In addition, the larger surface nominal area exhibited by f-GQDs provide the great opportunity to adsorb/immobilize agents targeting miRNA-21 and surviving, respectively. The combination of miRNA-21-targeting and surviving-targeting, improves the inhibition of cancer cell growth and apoptosis of cancer cells, significantly if compared with miRNA-21 and surviving, alone. These results provide a new versatile multifunctional nanocomposite, suitable for intracellular molecules analysis and also for clinical gene therapeutics.

The fourth case of study

Maji et al. [46], developed a new enzyme-mimetic nanostructured hybrid for *in vitro* detection and therapeutic treatment of cancer cells. The hybrid is prepared by the

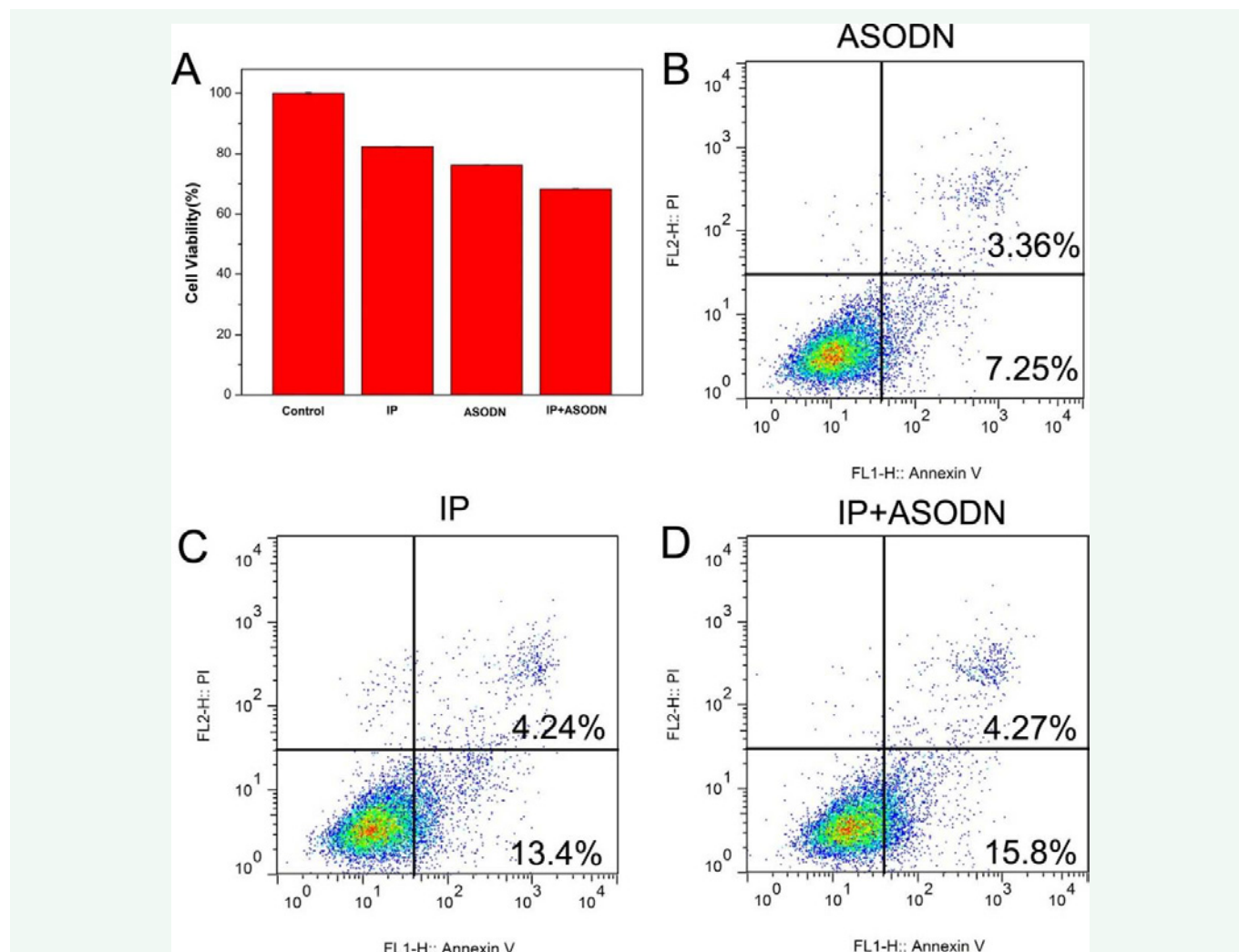


Figure 4 (A): Cell viability of HeLa cells transfected by f-GQDs/ASODN (14 $\mu\text{g}/\text{mL}$, 50 nM loaded ASODN), f-GQDs/IP (14 $\mu\text{g}/\text{mL}$, 50 nM loaded ASODN), and f-GQDs/IP/ASODN (14 $\mu\text{g}/\text{mL}$, 50 nM loaded ASODN and 50 nM IP). Flow cytometric apoptotic analysis of HeLa cell transfected by (B) f-GQDs/ASODN, (C) f-GQDs/IP, and (D) f-GQDs/IP/ASODN.

immobilization of gold nanoparticles (AuNPs) on mesoporous silica-coated nanosized reduced GO conjugated with Folic Acid (FA), a cancer cell-targeting ligand. The resulting nanostructured hybrid (labelled as GSF@AuNPs) exhibits an excellent peroxidase-like activity, detected by the catalytic oxidation of a typical peroxidase substrate, 3,3',5,5'-tetramethylbenzidine (TMB), in the presence of H_2O_2 . Prior to the anticancer activity of GSF@AuNPs, the toxicity of the new nanohybrid was measured using MTT (3-(4,5-dimethylthiazol-2-yl)-2,5-diphenyltetrazolium bromide) based assay, demonstrating negligible cytotoxicity effects. GSF@AuNPs hybrid catalyzes the conversion from H_2O_2 to $\text{OH}\cdot$ radical species. This reaction mechanism shows a concentration-dependent profile, based on a typical peroxidase-like enzymatic pathway, quite similar to that exhibited by iron oxide. GSF@AuNPs was found to possess superior peroxidase activity in acidic pH, which could be related to its anticancer activity by the generation of $\text{OH}\cdot$ radical in cancer cells when taking up into lysosomes.

According to these considerations, the nanohybrid is applied

as a selective, quantitative, and fast colorimetric detection tool for cancer cells. The improved catalytic activity of the GSF@AuNPs nanohybrid is related to the best combination of mesoporous silica-coated nanosized reduced GO (where reduced graphene conjugated with folic acid) composite material, that provides large surface area to increase the loading capacity of TMB on the hybrid through π - π stacking forces, while AuNPs is responsible for the catalytic chemical reaction. Furthermore, the mesoporous silica-coated nanosized reduced GO composite material represents a good nanoplatform for successful growth of well-dispersed small AuNPs without aggregation, preserving catalytic activities of AuNPs. The good stability and reproducibility of the GSF@AuNPs nanohybrid toward the catalytic oxidation of TMB were established using, five consecutive times, the hybrid for measurements.

To conclude, nanohybrids could be used for two main applications, that are, (1) selective, quantitative, and rapid colorimetric detection of cancer cells, as well as (2) cancer therapy by activating oxidative stress.

For what to concern the (1) application, a very well resolved color change has been recorded by the oxidation of TMB in the presence of GSF@ AuNPs for HeLa cancer cell. The calculated detection limit is about 50 cells, which could be visualized by the naked eye.

In the case of therapeutic treatments (application (2)), cancer cell damage occurs through the enhanced generation of OH• radical from exogenous H₂O₂ mediated by GSF@AuNPs nanoplatfrom. Instead of using exogenous H₂O₂, endogenous H₂O₂ produced by AA (Ascorbic Acid, that is a very well-known antioxidant reagent, and for decades it has widely used in cancer therapy) inside the cell cytoplasm was also feasible for the enhanced cell cytotoxicity against cancer cells. Both the detection and therapeutic processes are selective to cancer cells, indicating high specificity and robustness of the nanohybrid. Based on the simple peroxidase behavior, the developed hybrid would be a promising candidate for clinical cancer diagnostics and treatment.

The fifth case of study

Combination and integrated therapy can be defined as the simultaneous administration of two or more active therapeutics that are known to disrupt multiple targets, resulting in more efficient cancer treatments. The concept of multidrug delivery was utilized by Zhang et al. [47], by loading two anticancer drugs DOX and camptothecin (CPT) onto a folic acid GO carrier. Zhang et al. [47], report about Nanoscale Graphene Oxide (NGO) functionalized with sulfonic acid groups, and subsequently modified by the covalent binding of FA (i.e. FA-NGO). The resulting nanocomposite can specifically target the MCF-7 cells, that are human breast cancer cells which express FA receptors. Controlled loading of two anticancer drugs, doxorubicin (DOX) and camptothecin (CPT), on the FA-NGO new carrier, is investigated and experimental data show specific targeting to MCF-7 cells, and remarkably higher cytotoxicity compared to NGO loaded with DOX or CPT, without FA functionalization. The codelivery of both drugs shows a better target efficacy and higher cytotoxicity than GO loaded with DOX or CPT, alone respectively. Current chemotherapy for glioma is rarely satisfactory due to low therapeutic and efficiency and systemic side effects. A glioma-targeted drug delivery based on GO vector, was recently reported [48], in which targeted peptide chlorotoxin-conjugated graphene oxide were loaded with DOX. Cytotoxicity showed that chlorotoxin-conjugated GO/DOX mediated the highest rate of death of glioma cells compared with free DOX or GO loaded with DOX only. It is very well known that codelivery is an effective treatment of cancer and other pathological disorders.

Considering that the combination of two or more drugs is commonly used in polychemotherapy, and recently it seems to be very appealing and promising in nanobiomedicine, these graphene-based nanocomposites are eligible for several different applications.

DISCUSSION

This review reports on the synthetic routes to G and GD, on the characterization techniques, suitable for the univocal identification of G and graphene derivatives. Among of the

synthetic strategies, the electrochemical ones seem to be very promising especially in terms of mass production (i.e. scalability) and easy “one-step functionalization/engineering” of pG. Especially, two important properties, strongly influence the biocompatibility of pG, GO and GD, that are: the quality of graphene precursors (involved in the graphene synthesis, as described above in the full text); and the chemical, electrochemical and/or physical functionalization/engineering of graphene nano sheets.

For what to concern the high quality of the resulting graphene products, traditionally prepared GO often contains high concentrations of Mn²⁺ (97 ppm) and Fe²⁺ catalytic ions. It is very well known that both metals are highly mutagenic and nonspecific release of them from traditionally prepared graphene derivatives might result in unusually high levels of toxicity and damages of DNA. Consequently, researchers start to use Green Chemistry exfoliating methods. Recently, Peng et al. [49], report about a Fe²⁺-based green strategy, suitable for a production of a single layer of GO, in just 1 hour. Their approach resulted in the production of high purity GO containing 0.025 ppm of Mn²⁺ and 0.13 ppm Fe²⁺, respectively. The Patent N° PCTIB2016/053527 by Valentini F, as inventor, [50] describes a new electrochemical exfoliation mechanism of a Highly Oriented Pyrolytic Graphite working Anode, in an electrolytic bath, contained both exfoliating agents, such as: reduce glutathione (GSH) and alkaline phosphate (AP)-enzyme. This is a new green method because no heavy metals are involved, as catalysts, for the electrochemical growth/synthesis of graphene derivatives (which results in alkaline reduced graphene derivatives).

The cytotoxicity effects, studied in presence of graphene-based nanomaterials (*in vitro* test) remain conflicting (especially for GO and GD, final products) and they depend on the quality of the molecular/atomic precursors.

The second important aspect, related to the biocompatibility of carbon based nanomaterials, is the functionalization of the resulting products, that occurs on their surfaces, edges and sides. This aspect represent a future challenge for scientists because several different and conflicting opinions exist on the effects induced by different types of functionalized graphene. Here, in this paragraph, some examples are described. Previous studies examining the hemocompatibility of pG and GO demonstrated that pG shows a slightly higher cytotoxic effect than GO due to its strong hydrophobic interaction with cell membranes, [51]. Instead, Liao et al. [52], demonstrated that submicron-sized GO sheets induced the greatest hemolytic activity, whereas aggregated graphene sheets exhibited the lowest hemolytic activity. Coating GO nano sheets with chitosan almost eliminated hemolytic activity. It is possible to conclude that the toxicity of pG and GO depends on the exposure environment (ie, whether or not aggregation occurs) and mechanism of interaction with cell lines (ie, suspension versus adherent cell types).

In a recent investigation, Ding et al. [53], focus on the hemocompatibility of GO on human peripheral blood T lymphocytes and human serum albumin (HSA). In this work [53], the toxic mechanisms of pG, GO (mainly carboxylated GO-COOH) and GD (for example, GO-PEI/polyethyleneimine) to primary human peripheral blood T-lymphocytes and HAS, were studied.

pG seems to interact with the protein receptors to inhibit their ligand-binding capability, leading to ROS-dependent apoptosis through the B-cell lymphoma-2 (Bcl-2) pathway; GO (mainly carboxylated GO-COOH) exhibited a quite similar degree of toxicity on T lymphocytes except keeping a normal ROS level. Ding et al. [53], hypothesizes that GO-COOH inhibits protein-ligand binding and transfers the passive apoptosis signal to nucleus DNA through a ROS-independent pathway. GD (for example, GO-PEI/polyethyleneimine) exhibited serious hematotoxicity to T lymphocytes, provoking membrane disorders. The HSA binding with GO-COOH does not modify the HSA's binding capacity to bilirubin, while the binding of pG and GO-PEI provoke strong toxicity toward HSA.

Other authors, in literature [54], demonstrate that PEGylated GO, GO/PEI and GD exhibit certain advantages *in vitro* and *in vivo* drug delivery, such as high drug-loading efficacy, passive and active targeting capabilities, and reversal effects against cancer drug resistance. PEGylation and GO/PEI nanocomposites are known to enhance the solubility/better dispersibility of hydrophobic nanomaterials and these nanocomposites are widely used in nanomedicine [55]. Results show that incubation of several cells, as glioblastoma (U87MG), breast cancer cells (MCF-7), human ovarian carcinoma cell line (OVCAR-3), colon cancer cell (HCT-116), and lymphoblastoid cells (RAJI) with GO/PEG [56-58] exhibit no cytotoxicity up to 100 µg/mL. The capability of macrophages to entrap and remove graphene agents from the site of deposition enhances their biocompatibility. Mu et al. [59], confirmed that C2C12 progenitor cells used endocytosis mechanism to internalize medium-sized GO (500 nm) and phagocytosis for larger micron (1-2 µm)-sized sheets. Shortly after, both types of GO entered lysosomes for excretion. Almost no inhibition of cell proliferation was found at doses up to 100 µg/mL [59].

These different opinions in the literature [60], are probably related to poor-quality pG, GO and GD being used (broad lateral distributions >500 nm and the presence of contaminants, Mn²⁺, Fe³⁺, Cu²⁺, used as metal catalysts) and inconsistencies in assay design (MTT false positives and GO's strong autofluorescence signal).

Finally, there are many cautionary warnings in the literature [61], regarding the PEGylated forms of GO and its ROS production, in mammalian cell lines. Ceria (CeO₂) nanoparticles scavenge ROS and are eligible candidates for inclusion into a graphene-based vehicles [62]. According to this considerations, Kim et al. [63], reported a graphene-based multifunctional nanoplateform able to suppress ROS production. The multifunctional platform aligns plated cells and is suitable to perform *in situ* monitoring of cellular physiological characteristics, during proliferation and differentiation. Cell viability is represented by changes in impedance and monitored by an electrochemical instrumented cell-culture platform. Treatment with 5 M H₂O₂ in differentiated C2C12 cell lines provoked instant death in the majority of cells, resulting in a significant increase of the impedance output signals. Instead, the treatment with 5 mM H₂O₂ in the presence of Ceria (CeO₂), nanoparticles provoked only minimal changes in impedance electrochemical signals.

CONCLUSION AND FURTHER INVESTIGATION

This review focus on several aspects essential to consider for new nanomaterials, when they are applied as new nanocarriers in drug delivery. The key point is the synthetic strategies for graphene growth because they mainly influence all the resulting properties associated to the graphene final products. Chemical and Electrochemical synthetic strategies provide oxygenated functionalized graphene nanosheets. The characterization study (under a morphological/topographic and structural point of view) is a fundamental step to unequivocally identify graphene, with all the suitable characteristics, including the presence of structural defects, as the functional groups on nanosheet surfaces. Functionalization is essential to guarantee the best dispersibility of graphene nanosheets in the working cellular environment, and this is a crucial point for *in vitro* and *in vivo* experiments (improving the biodistribution of graphene in the cellular compartments). At the same time, functionalization carried out by the introduction of oxygenated functional groups (i.e., mainly COOH groups) could also provoke *in vitro* cytotoxicity on human cell lines. For this reason, to improve *in vitro* biocompatibility of graphene, used as nanocarrier of drugs and therapeutics, several different bio-coatings (i.e., mainly GO/PEI and GO/PEG nanocomposite materials) have been developed and detailed described herein. Many authors, cited in this review, show that the biopolymer coating increases cytotoxicity. At the state of the art, what can be proposed for graphene is a broad-spectrum study with different functionalized grafenes, tested on different human cell lines (normal and cancerous cell lines). In this way, it is possible to create a very useful database, able to explore the properties of graphene not only in the medical field but also with regard to the environmental impact and the safeguarding of the state of health, in the workplaces.

ACKNOWLEDGEMENTS

Authors wish to thank Smart Campus project (CUP E82I15000980002) and the INUIT Foundation, in Tor Vergata University, Roma, Italy for technical assistance and financial support.

REFERENCES

1. Wu L, Shan W, Zhang Z, Huang Y. Engineering nanomaterials to overcome the mucosal barrier by modulating surface properties. *Adv Drug Deliv Rev.* 2017.
2. Gao W, Chen Y, Zhang Y, Zhang Q, Zhang L. Nanoparticle-based local antimicrobial drug delivery. *Adv Drug Deliv Rev.* 2017.
3. Jeon IY, Choi HJ, Jung SM, Seo JM, Kim MJ, Dai L, et al. Large-Scale Production of Edge-Selectively Functionalized Graphene Nanoplatelets via Ball Milling and their Use as Metal-Free Electrocatalysts for Oxygen Reduction Reaction. *J Am Chem Soc.* 2013; 135: 1386-1393.
4. Yang G, Zhu C, Du D, Zhu J, Lin Y. Graphene-like two-dimensional layered nanomaterials: applications in biosensors and nanomedicine. *Nanoscale.* 2015; 7: 14217-14231.
5. Dutta S, Pati SK. Novel properties of graphene nanoribbons: a review. *J Mater Chem.* 2010; 20: 8207-8223.
- 6 (a). Geim AK. Graphene: Status and Prospects. *Science.* 2009; 324: 1530-1534.
- 6 (b). Novoselov KS. Nobel Lecture: Graphene: Materials in the Flatland.

- Rev Mod Phys. 2011; 83: 837.
- 6 (c). Geim AK. Nobel Lecture: Random walk to graphene. Rev Mod Phys. 2011; 83: 851.
 - 6 (d). Papageorgiou DG, Kinloch IA, Young RJ. Mechanical properties of graphene and graphene-based nanocomposites. Prog Mater Sci. 2017; 90: 75-127.
 7. Hummers WS, Offeman RE. Preparation of Graphitic Oxide. J Am Chem Soc. 1958; 80: 1339.
 8. Shahriary L, Athawale AA. Graphene Oxide Synthesized by using Modified Hummers Approach. Int J Renewable Energy and Environmental Engineering. 2014; 2: 58-63.
 9. Chen J, Yao B, Li C, Shi G. An improved Hummers method for eco-friendly synthesis of graphene oxide. Carbon NY. 2013; 64: 225-229.
 10. Chen J, Li Y, Huang L, Li C, Shi G. High-yield preparation of graphene oxide from small graphite flakes via an improved Hummers method with a simple purification process. Carbon N Y. 2015; 81: 826-834.
 11. Cataldo F, Compagnini G, Patane' G, Ursini O, Angelici, G, Ribic PR, et al. Graphene nanoribbons produced by the oxidative unzipping of single-wall carbon nanotubes. Carbon. 2010; 48: 2596-2602.
 12. Cataldo F, Compagnini G, D'Urso L, Palleschi G, Valentini F, Angelini G, et al. Characterization of graphene nanoribbons from the unzipping of MWCNTs. Fullerenes, Nanotubes, and Carbon Nanostructures. 2010; 18: 261-272.
 13. Parvez K, Wu ZS, Li R, Liu X, Graf R, Feng X, et al. Exfoliation of Graphite into Graphene in Aqueous Solutions of Inorganic Salts. J Am Chem Soc. 2014; 136: 6083-6091.
 14. Coleman JN. Liquid Exfoliation of Defect-Free Graphene. Acc Chem Res. 2013; 46: 14-22.
 15. Jinfeng C, Miao D, Guohua C. Continuous mechanical exfoliation of graphene sheets via three-roll mill. J Mater Chem. 2012; 22: 19625-19628.
 16. Chen F, Yang J, Bai T, Long B, Zhou X. Facile synthesis of few-layer graphene from biomass waste and its application in lithium ion batteries. J Electroanal Chem. 2016; 768: 18-26.
 17. Ruan G, Sun Z, Peng Z, Tour JM. Growth of Graphene from Food, Insects, and Waste. ACS Nano. 2011; 5: 7601-7607.
 18. Noushad M, Rahman IA, Sheeraz Che Zulkifli N, Husein A, Mohamad D. Low surface area nanosilica from an agricultural biomass for fabrication of dental nanocomposites. Ceram Int. 2014; 40: 4163-4171.
 19. Chen H, Wang W, Martin JC, Oliphant AJ, Doerr PA, Xu JF, et al. Extraction of Lignocellulose and Synthesis of Porous Silica Nanoparticles from Rice Husks: A Comprehensive Utilization of Rice Husk Biomass. ACS Sustain Chem Eng. 2013; 1: 254-259.
 20. Tay T, Ucar S, Karagöz S. Preparation and characterization of activated carbon from waste biomass. J Hazard Mater. 2009; 165: 481-485.
 21. Dias JM, Alvim-Ferraz MCM, Almeida MF, Rivera-Utrilla J, Sánchez-Polo M. Waste materials for activated carbon preparation and its use in aqueous-phase treatment: A review. J Environ Manage. 2007; 85: 833-846.
 22. Ojha K, Kumar B, Ganguli AK. Biomass derived graphene-like activated and non-activated porous carbon for advanced supercapacitors. J Chem Sci. 2017; 129: 397-404.
 23. Sharma M, Mondal D, Singh N, Prasad K. Biomass derived solvents for the scalable production of single layered graphene from graphite. Chem Commun (Camb). 2016; 52: 9074-9077.
 24. Shams SS, Zhang LS, Hu R, Zhang R, Zhu J. Synthesis of graphene from biomass: A green chemistry approach. Mater Lett. 2015; 161: 476-479.
 25. Saito R, Hofmann M, Dresselhaus G, Jorio A, Dresselhaus MS. Raman spectroscopy of graphene and carbon nanotubes. Adv Phys. 2011; 60: 413-550.
 26. Gupta A, Chen G, Joshi P, Tadigadapa S, Eklund PC. Raman scattering from high-frequency phonons in supported n-graphene layer films. Nano Lett. 2006; 6: 2667-2673.
 27. Ferrari AC, Meyer JC, Scardaci V, Casiraghi C, Lazzeri M, Mauri F, et al. Raman spectrum of graphene and graphene layers. Phys Rev Lett. 2006; 97: 187401.
 28. Lucchese MM, Stavale F, Ferreira Martins EH, Vilani C, Moutinho MVO, Capaz RB, et al. Quantifying ion-induced defects and Raman relaxation length in graphene. Carbon N Y. 2010; 48: 1592-1597.
 29. Wang G, Yang J, Park J, Gou X, Wang B, Liu H, et al. Facile Synthesis and Characterization of Graphene Nanosheets. J Phys Chem C. 2008; 112: 8192-8195.
 30. Krishnamoorthy K, Veerapandian M, Yun K, Kim SJ. The chemical and structural analysis of graphene oxide with different degrees of oxidation. Carbon NY. 2013; 53: 38-49.
 31. Pandey D, Reifengerger R, Piner R. Scanning probe microscopy study of exfoliated oxidized graphene sheets. Surf Sci. 2008; 602: 1607-1613.
 32. Johari P, Shenoy VB. Modulating Optical Properties of Graphene Oxide: Role of Prominent Functional Groups. ACS Nano. 2011; 5: 7640-7647.
 33. Liu K, Zhang JJ, Cheng FF, Zheng TT, Wang C, Zhu JJ. Green and facile synthesis of highly biocompatible graphene nanosheets and its application for cellular imaging and drug delivery. J Mater Chem. 2011; 21: 12034-12040.
 34. Yang D, Velamakanni A, Bozoklu G, Park S, Stoller M, Piner RD, et al. Chemical analysis of graphene oxide films after heat and chemical treatments by X-ray photoelectron and Micro-Raman spectroscopy. Carbon N Y. 2009; 47: 145-152.
 35. Syama S, Mohanan PV. Review: Safety and biocompatibility of graphene: A new generation nanomaterial for biomedical application. Int J Biol Macromol. 2016; 86: 546-555.
 36. Liu S, Zeng TH, Hofmann M, Burcombe E, Wei J, Jiang R, et al. Antibacterial Activity of Graphite, Graphite Oxide, Graphene Oxide, and Reduced Graphene Oxide: Membrane and Oxidative Stress. ACS Nano. 2011; 5: 6971-6980.
 - 37(a). Cheng C, Nie S, Li S, Peng H, Yang H, Ma L, et al. Biopolymer functionalized reduced graphene oxide with enhanced biocompatibility via mussel inspired coatings/anchors. J Mater Chem B. 2013; 1: 265-275.
 - 37(b). Cheng C, Li S, Nie S, Zhao W, Yang H, Sun S, et al. General and Biomimetic Approach to Biopolymer-Functionalized Graphene Oxide Nanosheet through Adhesive Dopamine. Biomacromolecules. 2012; 13: 4236-4246.
 38. Duch MC, Budinger GRS, Liang YT, Soberanes S, Urich D, Chiarella SE, et al. Minimizing Oxidation and Stable Nanoscale Dispersion Improves the Biocompatibility of Graphene in the Lung. Nano Lett. 2011; 11: 5201-5207.
 39. Chen Y, Qi Y, Tai Z, Yan X, Zhu F, Xue Q. Preparation, mechanical properties and biocompatibility of graphene oxide/ultrahigh molecular weight polyethylene composites. Eur Polym J. 2012; 48: 1026-1033.
 40. Xu M, Zhu J, Wang F, Xiong Y, Wu Y, Wang Q, et al. Improved *In Vitro*

- and *In Vivo* Biocompatibility of Graphene Oxide through Surface Modification: Poly(Acrylic Acid)-Functionalization is Superior to PEGylation. *ACS Nano*. 2016; 10: 3267-3281.
41. Zhang B, Wei P, Zhou Z, Wei T. Interactions of graphene with mammalian cells: Molecular mechanisms and biomedical insights. *Adv Drug Deliv Rev*. 2016; 105: 145-162.
 42. Mari E, Mardente S, Morgante E, Tafani M, Lococo E, Fico F, et al. Graphene Oxide Nanoribbons Induce Autophagic Vacuoles in Neuroblastoma Cell Lines. *Int J Mol Sci*. 2016; 17: 1995-2010.
 43. Chauhan G, Chopra V, Tyagi A, Rath G, Sharma RK, Goyal AK. "Gold nanoparticles composite-folic acid conjugated graphene oxide nanohybrids" for targeted chemo-thermal cancer ablation: *In vitro* screening and *in vivo* studies. *Eur J Pharm Sci*. 2017; 96: 351-361.
 44. Tian J, Luo Y, Huang L, Feng Y, Ju H, Yu BY. Pegylated folate and peptide-decorated graphene oxide nanovehicle for *in vivo* targeted delivery of anticancer drugs and therapeutic self-monitoring. *Biosens Bioelectron*. 2016; 80: 519-524.
 45. Dong H, Dai W, Ju H, Lu H, Wang S, Xu L, et al. Multifunctional Poly(L-lactide)-Polyethylene Glycol-Grafted Graphene Quantum Dots for Intracellular MicroRNA Imaging and Combined Specific-Gene-Targeting Agents Delivery for Improved Therapeutics. *ACS Appl Mater Interfaces*. 2015; 7: 11015-11023.
 46. Maji SK, Mandal AK, Nguyen KT, Borah P, Zhao Y. Cancer Cell Detection and Therapeutics Using Peroxidase-Active Nanohybrid of Gold Nanoparticle-Loaded Mesoporous Silica-Coated Graphene. *ACS Appl Mater Interfaces*. 2015; 7: 9807-9816.
 47. Zhang L, Xia J, Zhao Q, Liu L, Zhang Z. Functional Graphene Oxide as a Nanocarrier for Controlled Loading and Targeted Delivery of Mixed Anticancer Drugs. *Small*. 2010; 6: 537-544.
 48. Wang H, Gu W, Xiao N, Ye L, Xu Q. Chlorotoxin-conjugated graphene oxide for targeted delivery of an anticancer drug. *Int J Nanomedicine*. 2014; 18: 1433-1442.
 49. Peng L, Xu Z, Liu Z, Wei Y, Sun H, Li Z, et al. An iron-based green approach to 1-h production of single layer graphene oxide. *Nat Commun*. 2015; 6: 5716-5724.
 50. Patent N° PCTIB2016/053527
 51. Sasidharan A, Panchakarla LS, Sadanandan AR, Ashokan A, Chandran P, Girish CM, et al. Hemocompatibility and macrophage response of pristine and functionalized graphene. *Small*. 2012; 8: 1251-1263.
 52. Liao KH, Lin YS, Macosko CW, Haynes CL. Cytotoxicity of graphene oxide and graphene in human erythrocytes and skin fibroblasts. *ACS Appl Mater Interfaces*. 2011; 3: 2607-2615.
 53. Ding Z, Zhang Z, Ma H, Chen Y. *In vitro* hemocompatibility and toxic mechanism of graphene oxide on human peripheral blood T lymphocytes and serum albumin. *ACS Appl Mater Interfaces*. 2014; 6: 19797-19807.
 54. Sun XM, Liu Z, Welsher K, Robinson JT, Goodwin A, Zaric S, et al. Nanographene oxide for cellular imaging and drug delivery. *Nano Res*. 2008; 1: 203-212.
 55. Liu Z, Robinson JT, Sun X, Dai H. PEGylated nanographene oxide for delivery of water-insoluble cancer drugs. *J Am Chem Soc*. 2008; 130: 10876-10877.
 56. Feng L, Liu Z. Graphene in biomedicine: opportunities and challenges. *Nanomedicine*. 2011; 6: 317-324.
 57. Robinson JT, Tabakman SM, Liang Y, Wang H, Sanchez Casalongue H, Vinh D, et al. Ultrasmall reduced graphene oxide with high near-infrared absorbance for photothermal therapy. *J Am Chem Soc*. 2011; 133: 6825-6831.
 58. Chang Y, Yang ST, Liu JH, Dong E, Wang Y, Cao A, et al. *In vitro* toxicity evaluation of graphene oxide on A549 cells. *Toxicol Lett*. 2011; 200: 201-210.
 59. Mu Q, Su G, Li L, Gilbertson BO, Yu LH, Zhang Q, et al. Size-dependent cell uptake of protein-coated graphene oxide nanosheets. *ACS Appl Mater Interfaces*. 2012; 4: 2259-2266.
 60. Wu SY, Soo A, An S, Hulme J. Current applications of graphene oxide in Nanomedicine. *Int J Nanomedicine*. 2015; 10: 9-24.
 61. Yin PT, Shah S, Chhowalla M, Lee KB. Design, synthesis, and characterization of graphene-nanoparticle hybrid materials for bioapplications. *Chem Rev*. 2015; 115: 2483-2531.
 62. Karakoti A, Singh S, Dowding JM, Seal S, Self WT. Redox-active radical scavenging nanomaterials. *Chem Soc Rev*. 2010; 39: 4422-4432.
 63. Kim SJ, Cho HR, Cho KW, Qiao S, Rhim JS, Soh M, et al. Multifunctional cell-culture platform for aligned cell sheet monitoring, transfer printing, and therapy. *ACS Nano*. 2015; 9: 2677-2688.

Cite this article

Valentini F, Calcaterra A, Ruggiero V, Di Giacobbe M, Botta M, et al. (2018) Graphene as Nanocarrier in Drug Delivery. *JSM Nanotechnol Nanomed* 6(1): 1060.